Fixation and fate of C and N in the cyanobacterium *Trichodesmium* using nanometer-scale secondary ion mass spectrometry

Juliette A. Finzi-Hart[a,1,2], Jennifer Pett-Ridge[b,1], Peter K. Weber[b], Radu Popa[c], Stewart J. Fallon[d], Troy Gunderson[a], Ian D. Hutcheon[b], Kenneth H. Nealson[a], and Douglas G. Capone[a]

[a]Wrigley Institute for Environmental Studies and Department of Biological Sciences, University of Southern California, 3616 Trousdale Parkway, Los Angeles, CA 90089-0373; [b]Lawrence Livermore National Laboratory, PO Box 808, L-231, Livermore, CA 94551-0808; [c]Department of Biology, Portland State University, PO Box 751, Portland, OR 97207-0751; and [d]Research School of Earth Sciences, The Australian National University, Mills Road, Canberra ACT 0200, Australia

Edited by David M. Karl, University of Hawaii, Honolulu, HI, and approved February 20, 2009 (received for review October 22, 2008)

The marine cyanobacterium *Trichodesmium* is ubiquitous in tropical and subtropical seas and is an important contributor to global N and C cycling. We sought to characterize metabolic uptake patterns in individual *Trichodesmium* IMS-101 cells by quantitatively imaging ^{13}C and ^{15}N uptake with high-resolution secondary ion mass spectrometry (NanoSIMS). *Trichodesmium* fix both CO_2 and N_2 concurrently during the day and are, thus, faced with a balancing act: the O_2 evolved during photosynthesis inhibits nitrogenase, the key enzyme in N_2 fixation. After performing correlated transmission electron microscopy (TEM) and NanoSIMS analysis on trichome thin-sections, we observed transient inclusion of ^{15}N and ^{13}C into discrete subcellular bodies identified as cyanophycin granules. We speculate that *Trichodesmium* uses these dynamic storage bodies to uncouple CO_2 and N_2 fixation from overall growth dynamics. We also directly quantified both CO_2 and N_2 fixation at the single cell level using NanoSIMS imaging of whole cells in multiple trichomes. Our results indicate maximal CO_2 fixation rates in the morning, compared with maximal N_2 fixation rates in the afternoon, bolstering the argument that segregation of CO_2 and N_2 fixation in *Trichodesmium* is regulated in part by temporal factors. Spatial separation of N_2 and CO_2 fixation may also have a role in metabolic segregation in *Trichodesmium*. Our approach in combining stable isotope labeling with NanoSIMS and TEM imaging can be extended to other physiologically relevant elements and processes in other important microbial systems.

NanoSIMS | stable isotope labeling | cyanophycin

The marine cyanobacterium *Trichodesmium* is ubiquitous in tropical and subtropical seas and is an important contributor to global N and C cycling (1). As a diazotrophic cyanobacterium, *Trichodesmium* is capable of both CO_2 and N_2 fixation. Studies have estimated that it may leak up to 30–50% of its newly fixed N (2), providing a valuable source of bioavailable N to other nondiazotrophic phytoplankton species cohabitating in the N-limited subtropical gyres. Capone et al. (3) estimate that it contributes ≈5.7 Tmol new N y^{-1} in the North Atlantic Ocean, which is comparable with the rate of NO_3^- that diffuses from depth into oligotrophic upper ocean ecosystems (3, 4). Although *Trichodesmium* is not the sole diazotrophic cyanobacteria in the open ocean (5–7), it is the most conspicuous and well-studied. Also, it has been in culture since 1992 (8), allowing numerous studies of its physiology and response to different limiting and controlling factors. *Trichodesmium* is often included in ecosystem models that attempt to describe CO_2 and N_2 fixation in open ocean systems (9). A better understanding of CO_2 and N_2 fixation in *Trichodesmium* is critical, because this species has a large role in global C and N cycling in the open ocean.

Commonly referred to as "saw dust" on the surface of the sea (10), *Trichodesmium* grows in filaments (referred to as trichomes) that can have 100–200 cells (Fig. 1*B*). In the field, *Trichodesmium* may be found in its colony form, as either puff-shaped or tuft-shaped colonies (Fig. 1*A*) (11). Colonies typically have 100–200 trichomes. In some systems, free trichomes may predominate (12). *Trichodesmium* are high-light adapted, and have gas vesicles that keep them near the surface of the ocean (Fig. 1*C*) (13). They often form thick blooms visible in satellite imagery (14). *Trichodesmium* grown in culture usually occurs as free trichomes of ≈80–100 cells per trichome during exponential phase, and aggregates during stationary phase.

Diazotrophy is a significant challenge for unicellular microorganisms, because the O_2 produced from CO_2 fixation is inhibitory to nitrogenase, the key enzyme in N_2 fixation. Therefore, diazotrophs have developed different behavioral, biochemical, and physical strategies to protect nitrogenase from the O_2 evolved during photosynthesis. Certain cyanobacteria, such as *Gloeothece* spp., temporally segregate the processes over a diel cycle by fixing CO_2 during the day and fixing N_2 at night (15). Others, such as *Anabaena* spp., have terminally differentiated cells, termed heterocysts, with thickened cell walls, and reduced PS II and rubisco activity (16). These cells serve to spatially segregate the 2 processes, with N_2 fixation occurring in the heterocysts, whereas oxygenic photosynthesis and CO_2 fixation occurs in vegetative cells. *Trichodesmium* is unique in that it is a nonheterocystous cyanobacteria that fixes both CO_2 and N_2 concurrently during the day (1). There is considerable current debate among researchers as to how these processes co-occur. Current theories, and sometimes conflicting data, suggest increased O_2 consumption within cells protects nitrogenase [e.g., increased hydrogenase (17), Mehler (18, 19), and superoxide dismutase activity (20)], in addition to both spatial (21–23) and temporal segregation of CO_2 and N_2 fixation (19, 24, 25). Much of the current debate revolves around the metabolic potential of individual cells in a trichome, and how those capabilities may differ among cells in a trichome or within individual cells over time (26).

To investigate the dynamics of C and N metabolism at this level, we combined tracer-level additions of inorganic ^{13}C and ^{15}N with high-resolution secondary ion mass spectrometry (NanoSIMS; Cameca). NanoSIMS imaging allowed us to track C and N stable isotope incorporation rates and subsequent cellular fates by mapping distributions of isotopes (27) in multiple trichomes. The results of our NanoSIMS investigations are

Author contributions: J.A.F.-H., R.P., and D.G.C. designed research; J.A.F.-H., J.P.-R., P.K.W., S.J.F., and T.G. performed research; P.K.W., I.D.H., and K.H.N. contributed new reagents/analytic tools; J.A.F.-H., J.P.-R., and P.K.W. analyzed data; and J.A.F.-H., J.P.-R., P.K.W., and D.G.C. wrote the paper.

The authors declare no conflict of interest.

This article is a PNAS Direct Submission.

[1]J.A.F.-H. and J.P.-R contributed equally to this work.

[2]To whom correspondence should be addressed. E-mail: jahart@usc.edu.

This article contains supporting information online at www.pnas.org/cgi/content/full/0810547106/DCSupplemental.

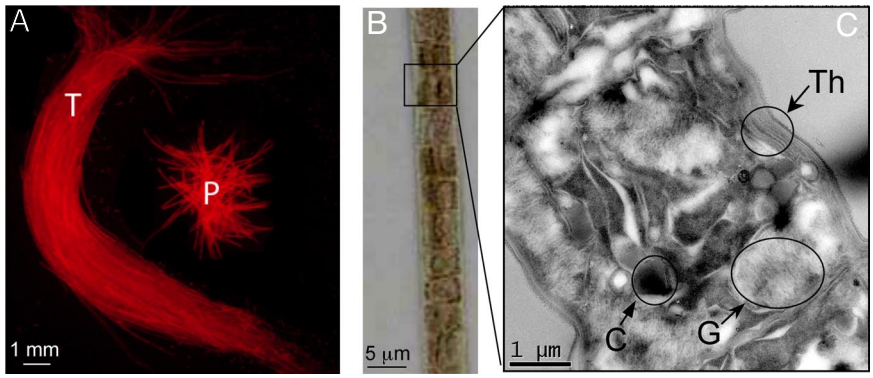

Fig. 1. Images of *Trichodesmium* filaments at 3 levels of magnification. (*A*) Image of *Trichodesmium* tuft (T) and puff (P) taken under green excitation (510–560 nm); (*B*) image of single *Trichodesmium* trichome by using light microscopy at 20× magnification; and (*C*) TEM image of individual *Trichodesmium* cell, demonstrating a cyanophycin granule (C), gas vesicles (G), and thylakoid membranes (Th).

compared with bulk isotopic analyses and related to existing models of *Trichodesmium* metabolism.

Results and Discussion

NanoSIMS imaging was performed on *Trichodesmium* trichomes spiked with $NaH^{13}CO_3$ and $^{15}N_2$, and harvested sequentially during 24 h (see *Materials and Methods*). Both whole- and thin-sectioned samples were imaged to quantify the distribution of newly fixed ^{13}C and ^{15}N within trichomes. The distribution of newly fixed ^{13}C and ^{15}N was determined by simultaneously imaging C and N isotopes and calculating quantitative $^{13}C/^{12}C$ and $^{15}N/^{14}N$ ratio images. Each 10-μm^2 image includes 2 to 3 cells, and was scanned with 150-nm resolution to capture intercellular variability. Multiple adjacent cells along multiple trichomes were analyzed to quantify cell–cell variability. For thin-sectioned trichomes, we used transmission electron microscopy (TEM) imaging to morphologically map samples before NanoSIMS analysis.

NanoSIMS analysis showed substantial subcellular spatial variability in ^{15}N and ^{13}C enrichment along *Trichodesmium* trichomes and with depth through individual cells (Figs. 2, 3, and 4); $^{13}C/^{12}C$ and $^{15}N/^{14}N$ ratio images generated from sectioned trichomes, along with correlated TEM maps, provide direct evidence of subcellular uptake localization within cells ≈8 h, and the redistribution of that enrichment after 24-h incubation (Fig. 3). In both sectioned and whole cells, we observed discrete hotspots enriched in ^{15}N and ^{13}C at 4 h, with increased density at 8 h (Figs. 2 *I* and *J*, and 3 *B* and *C*). These features are likely cyanophycin granules, a type of N-rich storage vacuole comprised of an asparagine and aspartate polymer found in many cyanobacteria (28–30), including *Trichodesmium* (21, 31). NanoSIMS analyses of *Trichodesmium* sections from 8 h indicate that

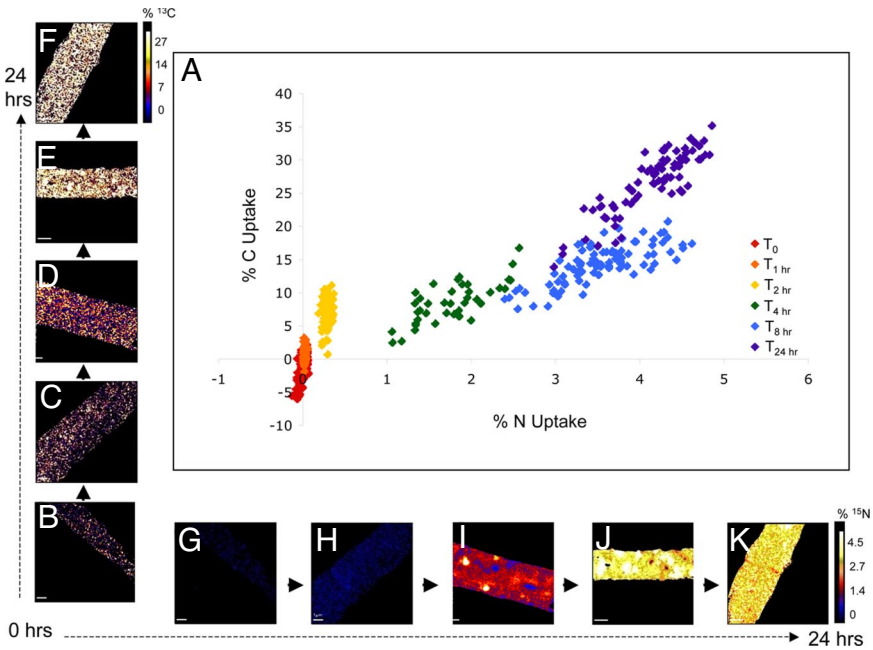

Fig. 2. Percentage ^{13}C and ^{15}N uptake by *Trichodesmium* trichomes at 6 time points and corresponding NanoSIMS images. (*A*) Percentage ^{13}C and ^{15}N uptake at 5 time points in *Trichodesmium* cells analyzed by NanoSIMS. Along the *x* axis are representative NanoSIMS images of ^{15}N enrichment in ≈2.5 cells at (*B*) 0 h, (*C*) 2 h, (*D*) 4 h, (*E*) 8 h, and (*F*) 24 h. Along the *y* axis are corresponding images of ^{13}C enrichment at (*G*) 0 h, (*H*) 2 h, (*I*) 4 h, (*J*) 8 h, and (*K*) 24 h. Data points represent average values for individual cells measured along a single trichome by NanoSIMS. [Scale bar, 1 μm; image enrichment scale ranges from 0 to 5% uptake (N), and 0 to 30% uptake (C), moving from black-blue-red-yellow-white.]

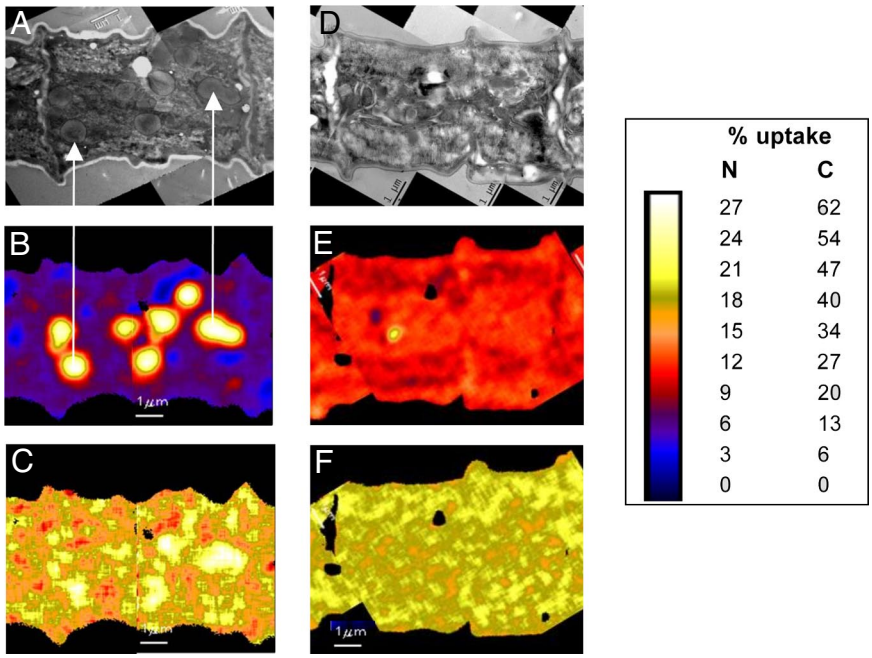

Fig. 3. TEM images of ≈2 cells from a *Trichodesmium* filament after (*A*) 8-h and (*D*) 24-h incubation with $H^{13}CO_3$ and $^{15}N_2$. Correlated NanoSIMS images demonstrate percentage fixed ^{15}N after (*B*) 8 h and (*E*) 24 h, percentage fixed ^{13}C after (*C*) 8 h and (*F*) 24 h. Arrows indicate correlation between cyanophycin granules identified by TEM and ^{15}N enriched hotspots evident in NanoSIMS image. (Scale bar, 1 μm.) Because NanoSIMS analysis is a destructive process, distinct cells were imaged for the 2 different time points.

the ^{13}C:^{15}N ratio of the cyanophycin granules is consistent with a mixture of asparagine (2:1) and aspartate (4:1), providing chemical evidence to identify these granules as cyanophycin. Also, these ^{15}N hotspots correspond directly to vacuole-like structures identified as cyanophycin granules in corresponding TEM images (Fig. 3 *A* and *B*). The hotspots were no longer evident after 24-h incubation, at which point cells were uniformly enriched with newly fixed ^{15}N (Figs. 2*K* and 3*E*). These results demonstrate the dynamic nature of these subcellular features, where it appears that newly fixed ^{15}N is stored during the daytime (when N_2 fixation is active), and is subsequently used at night for cellular biosynthesis (when N_2 fixation has ceased). As might be expected, elevated levels of ^{13}C are also associated with these cyanophycin granules (Fig. 3*C*).

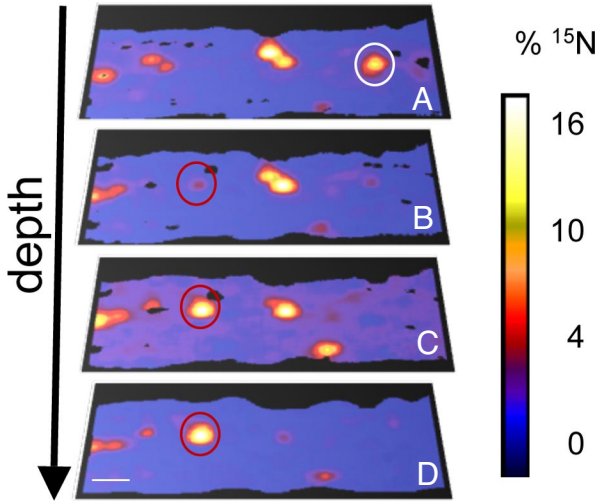

Fig. 4. Images of cyanophycin granules, as evidenced by hotspots of $^{15}N/^{14}N$ accumulation (percentage ^{15}N uptake), with depth through ≈2 individual cells. The white circle in *A* represents a cyanophycin granule that does not appear in the subsequent images. The red circles in *B–D* indicate a cyanophycin granule that becomes more prominent with depth through the cell. (Scale bar, 1 μm.)

NanoSIMS analysis also allowed us to examine subcellular isotope enrichment in the vertical dimension of cells. Based on analyses of multiple cells examined from multiple trichomes and time points, we determined that cyanophycin granules can comprise up to 6.4% (± 0.7%) of cell area/volume, and are evenly distributed along trichomes. In depth profile analyses of whole cells, as the NanoSIMS analyzed deeper and deeper layers, individual cyanophycin granules became apparent, and then disappeared as the ion beam sputtered through them (Fig. 4), suggesting that the granules are randomly distributed throughout the cell volume. It has been hypothesized that certain nondifferentiated cells, called "diazocytes", along a trichome contain nitrogenase and are the sole sites of N_2 fixation (21, 22, 32). Fredriksson and Bergman (21) found that only 24% of these diazocyte cells contained cyanophycin granules, compared with 61% of non-N_2-fixing cells. We did not find evidence for this theory in our samples. When cells were examined in TEM thin sections (0-, 8-, and 24-h incubations), and with NanoSIMS depth profiling (4- and 8-h incubations), cyanophycin granules were observed at similar densities in all cells.

Previous studies have examined the transient nature of cyanophycin granules in single-celled and heterocystous diazotrophs. Sherman et al. (30) used immunocytochemical analysis to demonstrate the localization of cyanophycin at the polar plugs of mature heterocysts in *Anabaena* sp. PCC7120. Mackerras et al. (33) used cultures of *Anabaena cylindrica* (a heterocystous cyanobacteria) and *Synechocystis* 6308 (a unicellular cyanobacteria that temporally segregates CO_2 and N_2 fixation) grown in media with limited ammonium concentration ($[NH_4^+]$). They demonstrate that synthesis and subsequent degradation of cyanophycin granules in these 2 organisms as $[NH_4^+]$ in the media is drawn down, indicating that the 2 cyanobacteria produce cyanophycin granules in N-replete conditions and use the stores

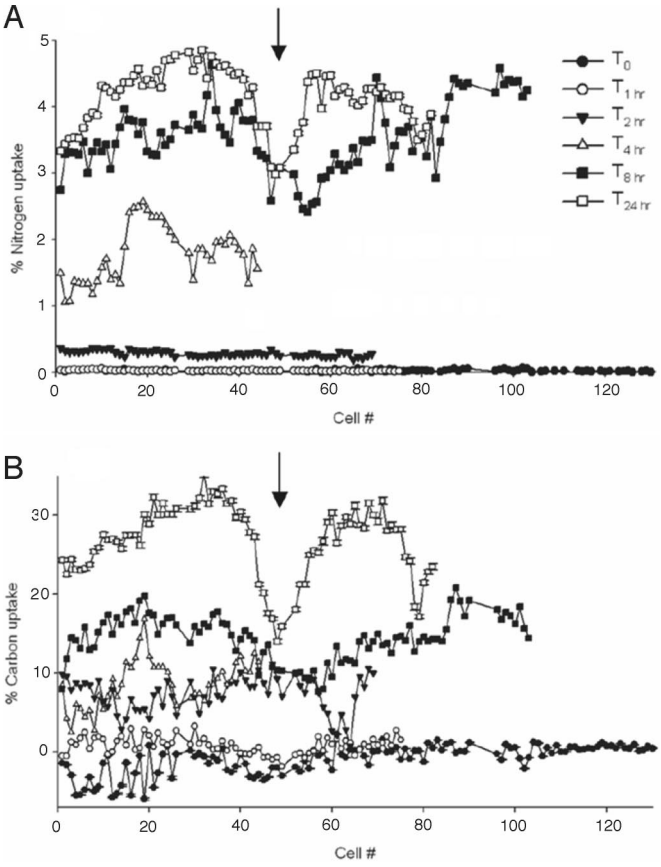

Fig. 5. Percentage isotope uptake in individual cells along the full length of *Trichodesmium* trichomes (filaments) at increasing time intervals for ^{15}N (*A*) and ^{13}C (*B*). Each data point represents average enrichment (measured by NanoSIMS) in a single cell, and data are plotted in the order found in the analyzed trichome. For example, the midpoint of the T_{24} trichome is found at approximately cell 50. Different symbols indicate trichomes from successive harvest points after addition of stable isotope labels. An arrow marks the point of proposed trichome division. Error bars represent 2 sigma error, but are small enough as to be obscured by the data symbols.

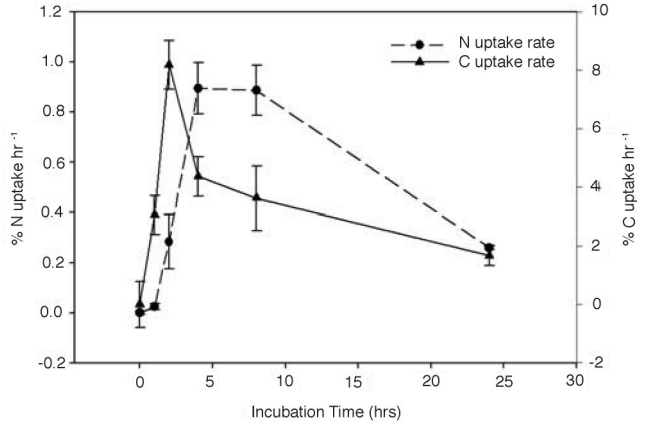

Fig. 6. ^{15}N and ^{13}C fixation rates (percentage uptake $hour^{-1}$) in *Trichodesmium* cells during a 24-h isotope labeling experiment. Data are generated from single cell NanoSIMS analysis of multiple filaments, and are averaged by time point (average $n = 73$ cells per time point). Error bars represent 2 sigma error.

during N-deplete conditions. Our study demonstrates the dynamic nature of the cyanophycin pool in *Trichodesmium* grown under diazotrophic conditions. Transient accumulation of cyanophycin indicates an uncoupling of CO_2 and N_2 fixation with cell growth. Interestingly, recent modeling of *Trichodesmium* metabolism (34) suggested that storage pools of C and N are dynamic over the diel cycle, accumulating during the day and consumed during the dark period. Our results provide direct evidence for this prediction.

In more than half of the trichomes analyzed from the 8- and 24-h incubations, we observed a marked reduction in ^{13}C and ^{15}N enrichment in cells located near the middle of trichomes (Fig. 5); this pattern may be related to programmed cell death (PCD) and/or trichome splitting. In *Trichodesmium*, as cells divide and the trichome increases in length, it is hypothesized that cells at the center of the trichome begin to have decreased metabolic activity and CO_2 and N_2 fixation. Eventually, the trichome splits at this point, yielding 2 shorter trichomes. Although PCD has been described for *Trichodesmium* (24, 35), we cannot confirm whether zones of reduced ^{13}C and ^{15}N uptake we observed are undergoing PCD, or whether the reduction in activity is due to other factors. However, secondary electron images we obtained before SIMS analysis provide visual evidence of thinner cells at these points (Fig. S1), suggesting that the trichome is stressed and about to break.

We used NanoSIMS analysis of whole cells to calculate uptake rates of CO_2 and N_2 fixation at the single cell level. These data were averaged for 40–120 contiguous cells located in multiple trichomes from each time point (Fig. 6), and were comparable to rates calculated from samples harvested in parallel, and bulk-analyzed by isotope ratio mass spectrometry (Fig. S2). Results from both approaches indicate that CO_2 fixation rates were highest in the morning (≈10 AM), whereas N_2 fixation rates were highest in the afternoon (≈12 PM; Fig. 6 and Fig. S2). These results provide evidence for a temporal decoupling of CO_2 and N_2 fixation in *Trichodesmium*, and corroborate earlier findings where Berman-Frank et al. (24) used fast repetition rate fluorescence (FRRF), O_2 production, $^{14}CO_2$ uptake, and acetylene reduction, to show maximal CO_2 fixation rates in the morning (≈11 AM) and afternoon (≈3 PM). Maximal N_2 fixation rates were measured at midday (≈12 PM), when CO_2 fixation was down-regulated. Küpper et al. (25), using fluorescence kinetic microscopy, provided further evidence for temporal segregation within individual cells, and suggest that there is a finely regulated shift between photosynthetic activity states throughout the course of the day that contributes to the protection of nitrogenase from O_2 evolved during photosynthesis. Together, our findings and these aforementioned studies build on the theory that increased O_2-consumptive activities within individual cells (17–20) enable them to temporally segregate the incompatible processes of CO_2 and N_2 fixation.

A controversial and evolving area of debate in the field of *Trichodesmium* physiology has been the suggestion that CO_2 and N_2 fixation within *Trichodesmium* are spatially segregated between different cells. The earliest microautoradiography studies suggested that spatial segregation happens at the level of the colony, with anoxic microzones occurring near the center of aggregates, where N_2 fixation was localized and photosynthesis down-regulated (36, 37). This theory was later questioned, when it was demonstrated that individual trichomes from disrupted colonies still fix both N_2 and CO_2 (38). More recently, conflicting immunochemical studies have examined the distribution of nitrogenase proteins along trichome cells. Some studies (23, 39) indicate that nitrogenase is dispersed throughout all cells in colonies, whereas other research suggests that only ≈15% of cells along a trichome contain nitrogenase (21, 22), and that these cells occur in clusters along the trichome (21, 32). These clusters, referred to as diazocytes, suggest a spatial segregation of N_2 fixation and CO_2 fixation. It should be noted that cells

that contain nitrogenase are not necessarily photosynthetically inactive (15).

In our study, after 2 h of exposure to labeled isotopes, newly fixed ^{13}C and ^{15}N was apparent and relatively evenly distributed in all cells along trichomes (Fig. 2). Although depleted regions did develop by 8 and 24 h, uptake of both C and N was simultaneously lower, and these regions corresponded to morphologically anomalous "thinning" spots thought to be prebreakage points (see discussion above). However, in our experiment, the lack of clear spatial differences in uptake patterns could be attributed to rapid redistribution of recently fixed C and N. Wolk et al. (40), using autoradiography with ^{13}N-N_2 gas, demonstrated in the cyanobacteria *Anabaena variabilis* that N_2 fixing cells are able to fix and redistribute newly fixed N to neighboring cells in <1.5 min. More recently, in experiments with the heterocystous cyanobacteria *Anabaena oscillariodes*, extant heterocysts were depleted in ^{15}N relative to vegetative cells (41), despite the fact that the heterocysts are the indisputable sites of N_2 fixation. This phenomenon may be due to the loss of diffusible ions and small molecules in the cytosol that are not fixed in place by cell fixatives used before NanoSIMS analysis (e.g., gluteraldehyde) (42). If a similar mechanism occurred in *Trichodesmium* cells, it could account for soluble metabolites formed in the early time points being undetectable. Although our data seems to suggest otherwise, it is possible that CO_2 and N_2 fixation did not occur concurrently within all cells.

Nonetheless, the accumulation of recently fixed ^{13}C and ^{15}N in individual cells appears uniform, and is significantly correlated with an average $r^2 = 0.4$ (Fig. 2), suggesting that these *Trichodesmium* trichomes do not contain diazocyte-like regions. We come to this conclusion by comparing our results with NanoSIMS analyses of *Anabaena* that contain specialized N_2-fixing heterocyst cells where the fate of recently fixed ^{13}C and ^{15}N is directly linked to cell physiology and development (41). In *Anabaena*, heterocysts fall outside the pattern of ^{13}C and ^{15}N correlation seen among vegetative cells (Fig. S3). If diazocyte cells of *Trichodesmium* behave similarly to heterocysts of *Anabaena*, and specialize in N_2 fixation at the expense of CO_2 fixation, we would expect to see a similar ^{13}C and ^{15}N anticorrelation in adjacent groups of *Trichodesmium* cells. In contrast, the relationship between ^{13}C and ^{15}N enrichment in *Trichodesmium* was consistent in all cells along a trichome at all time points. Because there are no groups of spatially adjacent cells that diverge from the mean in our *Trichodesmium* dataset, we take this result as evidence against specialized N_2 fixation regions (diazocytes), and conclude that temporal segregation may have a more dominant role in segregating CO_2 and N_2 fixation. However, the lack of observed enrichment at early (< 2 h) time points, and the possibility that rapid redistribution of enriched metabolites occurred between cells, precludes us from a firm conclusion on this important point. Studies using higher levels of isotope enrichment, in parallel with immunofluoretic methods, will hopefully provide a resolution to this current dilemma.

Conclusion

In summary, the NanoSIMS approach has allowed us to examine in detail the distribution and uptake ratio of CO_2 and N_2 in individual cells of a *Trichodesmium* trichome, and to compare patterns of distribution and uptake among cells in the trichome and over the diel cycle. We observed the uptake of newly fixed CO_2 and N_2 within all cells along a *Trichodesmium* trichome, as well as the dynamic nature of cyanophycin granules, which accumulate in cells during the light period and are metabolized and assimilated into cellular biomass during the dark period. These patterns suggest a temporal uncoupling of metabolic processes operating over the diel period in *Trichodesmium*. We have also provided direct evidence at a cellular level for a temporal decoupling of CO_2 and N_2 fixation in the trichome, with maximal CO_2 fixation occurring early in the day and maximal N_2 fixation occurring later in the day. We did not find evidence for specialized diazocyte cells; and if there is a "division of labor" in *Trichodesmium* trichomes, it is very transient, or occurs by some other mechanism. Unraveling the ecological and physiological complexities of this globally important organism remains an ongoing challenge. As present investigations reveal, a combined analysis approach, incorporating stable isotope labeling, modern imaging technologies (NanoSIMS, TEM, and SEM), and in situ molecular identification, may be critical to advanced studies of microbial metabolism.

Materials and Methods

Trichodesmium IMS-101 cultures were grown at 27 °C in 2-L polycarbonate culture bottles with YBCII liquid media (43) at an irradiance of 80 μE m^{-2} s^{-1} on a 12-h light/12-h dark cycle beginning at 8 AM. Subsamples of 165 mL were incubated in sealed 165 mL of serum vials. To each vial, we injected 0.07 mL $NaH^{13}CO_3$ (≈99 atom percentage ^{13}C, 0.04 M, final ^{13}C enrichment 1.9 atom percentage DIC; Cambridge Isotope Laboratories) and 0.3 mL 99 atom percentage $^{15}N_2$ gas (Isotech Associates) (final N_2 enrichment 16.2 atom percentage). There was no headspace in the bottles to ensure no dilution of the $^{15}N_2$ added with atmospheric $^{15}N_2$. Subsamples were returned to the incubator, and kept in the conditions described above until their predetermined harvest time. At 8 time points (0 min, 15 min, 30 min, 1 h, 2 h, 4 h, 8 h, and 24 h), 1 mL of sample was harvested and preserved in 2% glutaraldehyde for SIMS analysis. For the first time point (0 min), isotopes were injected, and then the sample was immediately harvested (i.e., within <30 s of injection). Experiments were initiated at 10 AM.

For NanoSIMS microanalysis, multiple whole *Trichodesmium* trichomes were filtered, washed with Milli-Q H_2O, and dried onto a silica chip. SIMS was performed at Lawrence Livermore National Laboratory by using a Cameca NanoSIMS 50 instrument, according to previously described methods (41). Briefly, a ≈2pA Cs^+ primary beam focused to ≈150 nm was scanned across a 256 × 256 pixel 10–15 μm^2 raster to generate secondary ions in ≈20 serial quantitative secondary ion images. Electron multiplier detectors collected $^{12}C^-$, $^{13}C^-$, $^{12}C^{14}N^-$, $^{12}C^{15}N^-$, and $^{31}P^-$ ions, and secondary electrons were simultaneously imaged. The NanoSIMS was tuned for ≈7,000 mass resolving power to resolve isobaric interferences. Samples were presputtered to at least 100 nm to achieve sputtering equilibrium; depth of measurement analysis ranged from 200 to 350 nm. For each time point, 4–5 trichomes were analyzed. We include data in Figs. 2 and 5 where we were able to analyze at least 40–120 contiguous cells. Data were processed as previously described (41) by using custom software. Briefly, each cell was defined as a region of interest using a 30% ^{12}C threshold; individual cells are easily identified in NanoSIMS secondary electron, ^{12}C and ^{14}N images. The isotopic composition for each ROI was calculated, corrected with reference standards, and converted to percentage uptake (Figs. 2 and 5) (41). Reference standards used included finely ground bovine liver (NIST SRM 1577b) (41) and a *Bacillus subtilis* spore preparation (44). Measurement precision, $\sigma_{(internal)}$, was 0.4–1.4% (2σ) for individual $^{13}C/^{12}C$ and $^{15}N/^{15}N$ measurements, and replicate analyses of the standard yielded an analytical precision, $s_{(std)}$, of 2.1% (2σ) for an individual measurement. Repeated measurements with depth on selected cells and on multiple filaments within a time point were used to ensure measurement accuracy. Rates of N and C fixation (Fig. 6) are the change C or N percentage uptake $hour^{-1}$ relative to the initial measurement. TEM analysis (Tecnai G2) was conducted on *Trichodesmium* filaments from the 0-, 8-, and 24-h time points, dehydrated in a series of ethanol washes, embedded in LR White epoxy, and microtomed to 150 nm. Correlated NanoSIMS analysis was then performed on the filaments imaged by TEM. Percentage area of cyanophycin granules were measured relative to whole-cell area in 65 cells from 6 distinct trichome thin-sections taken from the 0-, 8-, and 24-h time points. NanoSIMS analyses of *Anabaena* filaments (Fig. S3) are described in Popa et al. (41).

For each time point, a sample (50–75 mL) of bulk cell biomass was filtered onto precombusted GF/F filters and dried. The isotope ratio of these samples was analyzed at the University of Southern California Stable Isotope Facility on a VG IsoPrime interfaced to an elemental analyzer run in continuous flow mode.

ACKNOWLEDGMENTS. We thank John Waterbury (Wood Hole Oceanographic Institution, Woods Hole, MA) for providing us his *Trichodesmium* culture, IMS-101; Rachel Foster (University of California Santa Cruz) and Ed Carpenter (San Francisco State University) for their aid in identifying cyanophycin in the TEM images; Larry Nittler (Carnegie Institute of Washington) for software development; Christina Ramon [Lawrence Livermore National Lab-

oratory (LLNL)] for assistance with sample preparation for NanoSIMS and TEM analysis; and 3 anonymous reviewers, who provided valuable comments that helped improve the manuscript. This work was supported in part by the U.S. Department of Education Office of Biological and Environmental Research Genomics Genomes to Life Research Program (J.P.-R. and P.K.W.), and the National Science Foundation Ocean Science Program Grants OCE 0452765 and OCE 0753218. LLNL was supported by U.S. Department of Energy Contract DE-AC52-07NA27344.

1. Capone DG, Zehr J, Paerl H, Bergman B, Carpenter EJ (1997) Trichodesmium: A globally significant marine cyanobacterium. *Science* 276:1221–1229.
2. Glibert PM, Bronk DA (1994) Release of dissolved organic nitrogen by marine diazotrophic cyanobacteria, *Trichodesmium* spp. *Appl Environ Microbiol* 60:3996–4000.
3. Capone DG, et al. (2005) Nitrogen fixation by *Trichodesmium* spp.: An important source of new nitrogen to the tropical and sub-tropical North Atlantic Ocean. *Global Biogeochem Cycles* 19:GB2024.
4. Karl D, et al. (1997) The role of nitrogen fixation in biogeochemical cycling in the subtropical north Pacific ocean. *Nature* 388:533–538.
5. Zehr J, et al. (2001) Unicellular cyanobacteria fix N_2 in the subtropical North Pacific Ocean. *Nature* 412:635–638.
6. Falcón LI, Carpenter EJ, Cipriano F, Bergman B, Capone DG (2004) N_2 fixation by unicellular bacterioplankton from the Atlantic and Pacific Oceans: Phylogeny and in situ rates. *Appl Environ Microbiol* 70:765–770.
7. Montoya JP, et al. (2004) High rates of N_2-fixation by unicellular diazotrophs in the oligotrophic Pacific. *Nature* 430:1027–1031.
8. Prufert-Bebout L, Paerl HW, Lassen C (1993) Growth, nitrogen fixation and spectral attenuation in cultivated *Trichodesmium* species. *Appl Environ Microbiol* 59:1367–1375.
9. Hood RR, Christian JR (2008) *Nitrogen in the Marine Environment*, eds Capone DG, Bronk D, Mulholland M, Carpenter EJ (Elsevier, New York), pp 1445–1495.
10. Furnas M (1992) *Nitrogen in the Marine Environment*, eds Carpenter EJ, Capone DG (Academic, New York), pp 265–272.
11. Carpenter EJ, Subramaniam A, Capone DG (2004) Biomass and primary productivity of the cyanobacterium, *Trichodesmium* spp, in the southwestern tropical N Atlantic Ocean. *Deep-Sea Res PT I* 51:173–203.
12. Letelier RM, Karl DM (1996) Role of *Trichodesmium* spp. in the productivity of the subtropical north Pacific ocean. *Mar Ecol-Prog Ser* 133:263–273.
13. Carpenter EJ, Scranton MI, Novelli PC, Michaels A (1987) Validity of N_2 fixation rate measurements in marine *Oscillatoria* (*Trichodesmium*). *J Plankton Res* 9:1047–1056.
14. Carpenter EJ, Harvey HR, Fry B, Capone DG (1997) Biogeochemical tracers of the marine cyanobacterium *Trichodesmium. Deep-Sea Res* 44:27–38.
15. Gallon JR (1992) Reconciling the incompatible: N_2 fixation and O_2. Tansley Review No. 44. *New Phytol* 122:571–609.
16. Stewart WDP (1973) Nitrogen fixation by photosynthetic microorganisms. *Annu Rev Microbiol* 27:283–316.
17. Saino T, Hattori A (1982) Aerobic nitrogen fixation by the marine non-heterocystous cyanobacterium *Trichodesmium* (*Oscillatoria*) spp.: Its protective mechanism against oxygen. *Mar Biol* 70:251–254.
18. Kana TM (1993) Rapid oxygen cycling in *Trichodesmium thiebautii*. *Limnol Oceanogr* 38:18–24.
19. Milligan AJ, Berman-Frank I, Gerchman Y, Dismukes GC, Falkowski PG (2007) Light-dependent oxygen consumption in nitrogen-fixing Cyanobacteria plays a key role in nitrogenase protection 1. *J Phycol* 43:845–852.
20. Cunningham KA, Capone DG (1992) *Marine Pelagic Cyanobacteria: Trichodesmium and Other Diazotrophs*, ed Carpenter EJ (Kluwer Academic, Netherlands), pp 331–341.
21. Fredriksson C, Bergman B (1997) Ultrastructural characterisation of cells specialised for nitrogen fixation in a non-heterocystous cyanobacterium, *Trichodesmium* spp. *Protoplasma* 197:76–85.
22. Lin S, Henze S, Lundgren P, Bergman B, Carpenter E (1998) Whole-cell immunolocalization of nitrogenase in marine diazotrophic cyanobacteria, *Trichodesmium* spp. *Appl Environ Microbiol* 64:3052–3058.
23. Ohki K (2008) Intercellular localization of nitrogenase in a non-heterocystous cyanobacterium (cyanophyte) *Trichodesmium* sp. NIBB1067. *J Oceanogr* 64:211–216.
24. Berman-Frank I, et al. (2001) Segregation of nitrogen fixation and oxygenic photosynthesis in the marine cyanobacterium *Trichodesmium. Science* 294:1534–1537.
25. Küpper H, Ferimazova N, Setlik I, Berman-Frank I (2004) Traffic lights in Trichodesmium. Regulation of photosynthesis for nitrogen fixation studied by chlorophyll fluorescence kinetic microscopy. *Plant Physiol* 135:2120–2133.
26. Bergman B (1999) *Marine Cyanobacteria*, eds Charpy L, Larkum T (Institute Oceanographic, Monaco), Vol 19, pp 158–163.
27. Lechene C, et al. (2006) High-resolution quantitative imaging of mammalian and bacterial cells using stable isotope mass spectrometry. *J Biol* 5:20.
28. Simon RD (1987) *The cyanobacteria.* (Elsevier, Amsterdam), pp. 199–225.
29. Simon RD (1971) Cyanophycin granules from the blue-green alga *Anabaena cylindrica*: A reserve material consisting of copolymers of aspartic acid and arginine. *Proc Natl Acad Sci USA* 68:265–267.
30. Sherman DM, Tucker D, Sherman LA (2000) Heterocyst development and localization of cyanophycin in N_2-fixing cultures of *Anabaena* sp. PCC7120 (Cyanobacteria). *J Phycol* 36:932–941.
31. Romans KM, Carpenter EJ, Bergman B (1994) Buoyancy regulation in the colonial diazotrophic cyanobacterium *Trichodesmium tenue*: Ultrastructure and storage of carbohydrate, polyphosphate and nitrogen. *J Phycol* 30:935–942.
32. El-Shehawy R, Lugomela C, Ernst A, Bergman B (2003) Diurnal expression of hetR and diazocyte development in the filamentous non-heterocystous cyanobacterium *Trichodesmium erythraeum. Microbiology* 149:1139–1146.
33. Mackerras AH, Youens BN, Weir RC, Smith GD (1990) Is cyanophycin involved in the integration of nitrogen and carbon metabolism in the cyanobacteria *Anabaena cylindrica* and *Gloeothece* grown on light/dark cycles? *Gen Microbiol* 136:2049–2056.
34. Rabouille S, Staal M, Stal L, Soetaert K (2006) Modeling the dynamic regulation of nitrogen fixation in the cyanobacterium *Trichodesmium* sp. *Appl Environ Microbiol* 72:3217–3227.
35. Berman-Frank I, Bidle KD, Haramaty L, Falkowski PG (2004) The demise of the marine cyanobacterium, *Trichodesmium* spp, via an autocatalyzed cell death pathway. *Limnol Oceanogr* 49:997–1005.
36. Carpenter EJ, Price CC (1976) Marine Oscillatoria (*Trichodesmium*): Explanation for aerobic nitrogen fixation without heterocysts. *Science* 191:1278–1280.
37. Paerl HW (1994) Spatial segregation of CO_2 fixation in *Trichodesmium* spp.: Linkage to N_2 fixation potential. *J Phycol* 30:790–799.
38. Carpenter EJ, et al. (1990) Re-evaluation of nitrogenase oxygen-protective mechanisms in the planktonic marine cyanobacterium *Trichodesmium. Mar Ecol-Prog Ser* 65:151–158.
39. Paerl HW, Priscu JC, Brawner DL (1989) Immunochemical localization of nitrogenase in marine *Trichodesmium* aggregates: Relationship to N_2 fixation potential. *Appl Environ Microbiol* 55:2965–2975.
40. Wolk CP, Austin SM, Bortins J, Galonsky A (1974) Autoradiographic localization of ^{13}N after fixation of ^{13}N-labeled nitrogen gas by a heterocyst-forming blue-green alga. *J Cell Biol* 61:440–453.
41. Popa R, et al. (2007) Carbon and nitrogen fixation and metabolite exchange in and between individual cells of *Anabaena oscillarioides. ISME J* 1:354–360.
42. Guerquin-Kern JL, Wu TD, Quintana C, Croisy A (2005) Progress in analytical imaging of the cell by dynamic secondary ion mass spectrometry (SIMS microscopy). *BBA-Gen Subjects* 1724:228–238.
43. Chen YB, Zehr JP, Mellon M (1996) Growth and nitrogen fixation of the diazotrophic filamentous nonheterocystous cyanobacterium *Trichodesmium* sp IMS 101. *J Phycol* 32:916–923.
44. Behrens S, et al. (2008) Linking microbial phylogeny to metabolic activity at the single-cell level by using enhanced element labeling-catalyzed reporter deposition fluorescence in situ hybridization (EL-FISH) and NanoSIMS. *Appl Environ Microbiol* 74:3143–3150.